"Mining Minima": Direct Computation of Conformational Free Energy

Martha S. Head, James A. Given, and Michael K. Gilson*

Center for Advanced Research in Biotechnology, National Institute of Standards and Technology, 9600 Gudelsky Drive, Rockville, Maryland 20850

Received: November 15, 1996[⊗]

We describe a novel, two-step method for directly computing the conformational free energy of a molecule. In the first step, a finite set of low-energy conformations is identified, and its contribution to the configuration integral is evaluated by a straightforward Monte Carlo technique. The method of finding energy minima incorporates certain features of the global-underestimator method and of a genetic algorithm. In the second step, the contribution to the configuration integral due to conformations not included in the initial integration is determined by Metropolis Monte Carlo sampling. Applications to alanine oligopeptides and to three cyclic urea inhibitors of HIV protease are presented.

Introduction

Many applications in computational chemistry involve computing the relative stability of two different conformational states of a molecular system. For example, one may wish to determine the relative stability of two different conformations of a single molecule, or the standard free energy of binding for a host−guest system or a protein−ligand complex. Methods for computing the free energy of binding are particularly important because of their applicability to computer-aided drug design.

For computer models in which the solvent is treated explicitly, the most commonly used methods for computing relative free energies are perturbative methods, such as free energy perturbation (FEP) or multiconfigurational thermodynamic integration (MCTI).[1−6] In these methods, a system is perturbed in small steps from one state to another and the work of carrying out each step is summed to yield the work—or the change in free energy—for the entire process. This is an elegant approach, but it is often prohibitively slow, for at least two reasons. First, the explicit treatment of solvent molecules is time-consuming in general. Second, perturbative methods require equilibration of the system at each step of the transformation from one state to another.

The recent successes of implicit solvent models[7−12] motivate the development of methods for computing free energy differences that exploit the computational speed of these approaches. Perturbative methods such as FEP and MCTI could be used with implicit solvent models. However, it seems reasonable to expect greater speed from methods that do not require the system to be equilibrated for a number of perturbative steps. Several groups have presented nonperturbative methods and have obtained promising results.[13−18]

In the studies of June *et al.*[13] and Maginn *et al.*,[14] the value of Henry's constant is calculated for alkanes in zeolite pores. The requisite configuration integrals are computed by Monte Carlo integration, with structures generated by a configuration bias technique to improve convergence. Two other methods[15−18] calculate free energies by summing over local energy minima. The method of Lipkowitz *et al.*[15,16] involves summing the Boltzmann factor of a single conformation at each energy minimum. This method implicitly assumes that the different energy minima have exactly the same shape and are separated by high-energy barriers. The method of Wang *et al.*[17,18] includes more information about the shape of the energy surface, using a systematic search of conformation space to assign an approximate width to each energy well. However, the method approximates all energy minima as harmonic wells separated by large energy barriers. We are not aware of any efforts to examine the validity of the approximations in existing methods based on sums over minima.

We find these methods promising and present a novel "mining-minima" algorithm for directly computing the configuration integral of a molecule as the sum of the contributions of low-energy states. No assumptions are made concerning the size and shape of potential energy wells. The method of locating energy minima is novel and incorporates key features of the global-underestimator method of Phillips *et al.*[19] and of genetic algorithms. We also introduce a free energy correction for conformational states not sampled by the integration over energy minima. This correction is in the spirit of the predominant-states method developed in a different context[20] and of a recently described approximation to configuration integrals of small molecules.[21,22] The accuracy of the new method is assessed by test calculations on a series of molecules of various sizes.

Theory

Conformational Free Energy. We are interested in computing the chemical potential of a molecule in solution. It can be shown that, in the classical approximation to statistical thermodynamics, the standard chemical potential at constant volume equals[23,24]

$$\mu^\circ = -RT \ln\left(\frac{8\pi^2}{\sigma_{\text{ext}} C^\circ}\right) - RT \ln Z \qquad (1)$$

Here σ_{ext} is the symmetry number for external symmetry operations which leave internal coordinates of the molecule unchanged, C° is the standard concentration, and Z is the configuration integral over the internal coordinates of the molecule. A term that depends upon atomic masses is omitted here, because it will cancel as soon as the difference is taken between two chemical potentials for the same molecule. For a molecule with n atoms, Z is given by

$$Z \equiv \frac{1}{\sigma_{\text{int}}} \int_0^{2\pi} \prod_{i=1}^{n-3} \mathrm{d}\phi_i \int_0^{\pi} \prod_{j=1}^{n-2} \mathrm{d}\theta_j \int \prod_{k=1}^{n-1} \mathrm{d}\rho_k \times J(\{\theta,\rho\}) \mathrm{e}^{-(U(\{\phi,\theta,\rho\})+W(\{\phi,\theta,\rho\}))/RT} \qquad (2)$$

* To whom correspondence should be addressed. E-mail: gilson@indigo14.carb.nist.gov.

[⊗] Abstract published in *Advance ACS Abstracts,* February 1, 1997.

S1089-5639(96)03817-0 CCC: $14.00

Here the internal coordinates of the molecule are given in terms of $n - 3$ torsion angles $\{\phi_i\}$, $n - 2$ bond angles $\{\theta_j\}$, and $n - 1$ bond lengths $\{\rho_k\}$.[25] The integration over bond lengths is restricted to values of ρ_k consistent with molecular bonds remaining intact.[26] The Jacobian determinant for the transformation from Cartesian to internal coordinates, $J(\{\theta,\rho\})$, does not depend upon $\{\phi_i\}$.[14] The configuration integral defined here includes the symmetry number σ_{int} to account for internal symmetries due to rotations about classical bonds. For example, in addition to an external symmetry number σ_{ext} of 2, an ethane molecule has an internal symmetry number σ_{int} of 9 due to rotations of methyl groups. The overall symmetry of ethane, $\sigma = \sigma_{\text{ext}}\sigma_{\text{int}}$, is therefore 18.[27] The energy in the Boltzmann factor is written as the sum of a vacuum potential energy U and of a solvent term W that equals the work of transferring the molecule from vapor phase to solvent in a fixed conformation. Curly brackets, { }, indicate a full set of coordinates of the specified types.

In what follows, it will be assumed that an adequate approximation to changes in free energy can be obtained by integrating over only the "soft" internal degrees of freedom, *i.e.*, the m torsion angles lacking significant double-bond character. This will be a good approximation so long as the conformational transformations considered do not significantly alter the probability distribution of the neglected "hard" degrees of freedom.[24] Furthermore, the "hard" degrees of freedom are expected to require a quantum, rather than a classical, treatment. Also, in the present paper, solvent effects are treated only by simple dielectric screening models. In effect, $U + W$ is replaced by an energy function E consisting of the vacuum force field evaluated with a dielectric constant greater than or equal to 1. With these simplifications, the configuration integral may be rewritten as

$$Z \approx C\, Z_{\text{tor}} \tag{3}$$

$$Z_{\text{tor}} \equiv \frac{1}{\sigma_{\text{int}}}\int_0^{2\pi} \mathrm{e}^{-E(\{\phi\})/RT} \prod_{i=1}^{m} \mathrm{d}\phi_i \tag{4}$$

where C is a constant that results from integration over the "hard" degrees of freedom. In what follows, we will speak of the "conformational free energy" $A_{\text{tor}} \equiv -RT \ln Z_{\text{tor}}$. Note, however, that the "mining-minima" method can readily be generalized to include the neglected degrees of freedom and more sophisticated solvent models.

Monte Carlo Integration. The conformational free energy, A_{tor}, can be rewritten as[28]

$$A_{\text{tor}} = -RT \ln\left[\frac{V}{\sigma_{\text{int}}}\langle \mathrm{e}^{-E(\{\phi\})/RT}\rangle\right] \tag{5}$$

where $V = (2\pi)^m$ is the volume of conformation space and the angle brackets represent an unweighted mean of the Boltzmann factor over conformation space. In what follows, the internal symmetry number σ_{int} is not included explicitly. Instead, internal symmetries are accounted for by computing the mean Boltzmann factor over a subset of the conformation space of relevant dihedral angles. For example, for rotations about methyl dihedrals, the mean is computed for the dihedral range $[0, 2\pi/3]$, and the requisite change is made to the volume term.

The unweighted average in eq 5 may be evaluated numerically as an average over a large number N of randomly generated conformations of the molecule:

$$A_{\text{tor}} \approx A_{\text{MC}} \equiv -RT \ln\left[\frac{V}{N}\sum_{i=1}^{N} \mathrm{e}^{-E_i/RT}\right] \tag{6}$$

where A_{MC} is the conformational free energy computed by Monte Carlo (MC) integration and E_i is the potential energy evaluated for conformation i having torsion angles $\{\phi_i\}$. Equation 6 gives a prescription for the direct computation of conformational free energy. For a given molecule, one randomly generates a large number of conformations spread uniformly throughout the integration volume, calculates the average Boltzmann factor, and multiplies by the volume of the space. Note that this Monte Carlo integration approach differs from commonly used Monte Carlo algorithms, such as that of Metropolis *et al.*,[29] which yield a Boltzmann distribution of conformations, but do not yield an actual configuration integral.

The challenge in this method is achieving adequate sampling over what may be a very large volume of conformational space. As demonstrated below, eq 6 can be used to compute converged numerical values of A_{MC} for small molecules with few degrees of torsional freedom. For larger molecules, the convergence and accuracy of the calculation can be improved by spending more computational effort in areas of the integration volume where the value of the Boltzmann factor is large. A method for doing this is now described.

Predominant States. The predominant-states approximation[20] uses the fact that the largest contributions to the configuration integral are found in and near energy minima, because the Boltzmann factors are largest at these minima. The complete configuration integral is therefore approximated from the free energy contributions A_j of a finite number M of potential energy wells j. Thus,

$$A_{\text{tor}} \approx A_{\text{MM}} \equiv -RT \ln \sum_{j=1}^{M} \mathrm{e}^{-A_j/RT} \tag{7}$$

where

$$A_j \approx -RT \ln\left[\frac{v_j}{N_j}\sum_{i=1}^{N_j} \mathrm{e}^{-E_i/RT}\right] \tag{8}$$

and A_{MM} is the conformational free energy computed by the mining-minima algorithm described in detail below. Here, v_j is the volume of configuration space sampled for energy well j, and N_j is the number of random conformations generated during MC integration of well j.

Correction for Other Conformations. For potential energy landscapes in which the free energy is dominated by a small number of very low-energy states, the predominant-states calculation outlined above will provide well-converged free energy values. However, for systems with many degrees of freedom, and for those with smooth energy landscapes, the configuration integral is generally not dominated by a small number of low-energy states. Instead, an extremely large volume of configuration space makes a non-negligible contribution to the overall free energy. As a consequence, the predominant-states calculation is slow to converge and may ignore important contributions from relatively high-energy states.

In such cases, the results can be corrected by using a Metropolis Monte Carlo method in the entire conformational space to compute the fractional occupancy, f_M, of the M states that have been sampled. Then, as previously shown,[20−22] the

corrected free energy $A_{MM,corr}$ is given by

$$A_{MM,corr} = A_{MM} + RT \ln(f_M) \quad (9)$$

It is thus possible to correct for conformations not included in the M energy minima if f_M can be computed with sufficient accuracy.

Methodology

The mining-minima methodology involves locating minimum energy structures and computing A_{MM}. Then a Metropolis Monte Carlo simulation is carried out in order to calculate the fractional occupancy, f_M, of the portion of phase space occupied by the M energy minima. The method is illustrated here for alanine dipeptide. The example calculations were carried out using a locally modified version of UHBD,[30] the CHARMM 22 parameter set,[31] and a constant dielectric, $\epsilon = 25.0$. This particular calculation is used merely for illustrative purposes, so no attempt has been made to optimize the computations involved. The results of more challenging cases are presented in the Results and Discussion section.

Integrating over Energy Minima. Calculation of A_{MM} is an iterated, three-step process. First, a new local energy minimum is identified. Second, the extent of the associated potential energy (PE) well is determined. Third, the free energy of the PE well is calculated by Monte Carlo integration. This procedure is repeated until a convergence criterion is satisfied.

Finding a Local Minimum Structure. The conformation of the molecule being analyzed is specified by a set of m dihedral angles. Minimum energy conformations are identified by a novel algorithm, termed "anamnestic" because it uses the memory of previously found minima to speed convergence. The procedure is as follows.

In the early stages of "anamnestic" sampling, random dihedral angle values $\{\phi_i\}$ are generated within the range $[-\pi, \pi]$ for dihedrals with no internal symmetry, and the potential energy of each conformation is computed. Dihedral angle values are generated in a restricted range for internally symmetric dihedrals; for example, methyl dihedral angles are generated in the range $[0, 2\pi/3]$. As sampling proceeds, conformations are generated with torsion angles that lie in a gradually decreasing range about the current minimum PE structure, thereby narrowing in on a local energy minimum. Any time a new conformation is more stable than the existing energy minimum, the center of the sampling range is moved to the new energy minimum. This procedure is motivated by the idea that it makes sense to seek low-energy structures in regions where relatively low energy structures have already been found. Once the sampling range narrows to zero, a local energy minimum $\{\Phi_i\}$ has been located. This local minimum is stored for use in later cycles of anamnestic sampling.

This procedure is related to the global-underestimator method of Phillips *et al.*[19] The global-underestimator method constructs a quadratic function that approximates and underlies a set of previously located local minima. The method assumes that the global energy minimum lies near the minimum of this quadratic function. Therefore, a new set of local energy minima is generated in the vicinity of the minimum of the quadratic function. A new global estimator is generated from these minima, and the process iterates to convergence. However, it is likely that the minimum of the global underestimator will, in fact, be near the lowest energy structure in the set of local minima used to define the underestimator. Therefore, in the present study, the global underestimator is not used. Instead, the search simply focuses on the lowest energy conformation found so far.

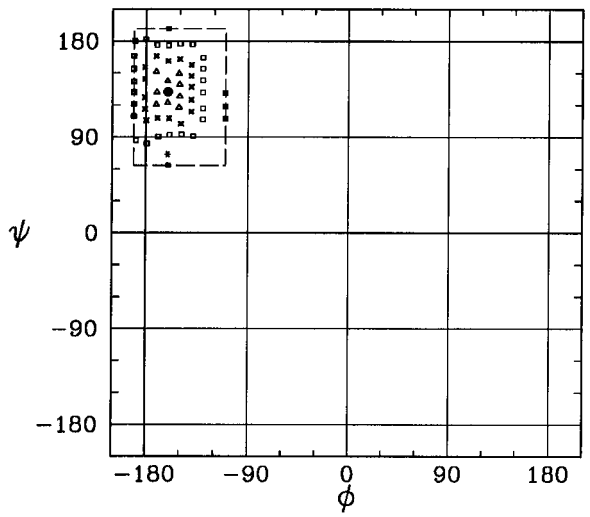

Figure 1. First PE well of alanine dipeptide. The large, filled circle indicates the location of the global minimum of alanine dipeptide for calculations carried out at $\epsilon = 25$. The other marked points indicate low-energy structures located as subsequent hypershells are sampled. An energy cutoff of 42 kJ/mol above the minimum PE was used in this calculation. The dashed line represents the extent of the PE well.

The present method is enhanced by allowing newly generated conformations a finite probability of using some torsion angles from the structures of stored energy minima $\{\Phi_i\}$. The idea is that different local energy minima may be similar to each other. It therefore makes sense to use previously located minimum structures as partial solutions when proposing new conformations. This feature of the present method is similar in spirit to the possibility of a crossover mutation in a genetic algorithm,[32−36] and was found to markedly improve the ability of the present method to find deep minima quickly. Repeated cycles of anamnestic sampling will rapidly locate a deep local minimum with energy $E_{min,j}$. For alanine dipeptide, the first minimum found—shown as a large filled circle in Figure 1—was the global minimum at $\phi = -160$ and $\psi = 132$. The performance of this minimizer on more complex systems is discussed below.

Determining the Extent of the PE Well. Given a minimum PE structure, successive m-dimensional rectangular hypershells about the minimum are sampled in order to locate low-energy structures that are nearby in dihedral space. Low-energy structures within a hypershell are located by anamnestic sampling, with the following constraints. First, only structures below a given potential energy cutoff E_{cutoff} relative to the energy $E_{min,j}$ at the base of the well are retained. Second, low-energy structures within a hypershell are not allowed to be closer to each other than a specified excluded dihedral range. In practice, this criterion means that two low-energy structures must differ by more than the excluded range in at least one dihedral angle. This excluded-range criterion prevents the bottom of the energy well from being rediscovered repeatedly and allows "mining" of the PE well for *different* low-energy structures, thereby identifying the extent of the well.

Sampling in the hypershells around a given energy minimum is terminated under two conditions. First, sampling ceases when no new structures are found with potential energy below a fixed $E_{min,j} + E_{cutoff}$. The example calculation presented here uses an energy cutoff of 42 kJ/mol. Alternatively, sampling ceases when structures in a hypershell descend into a different PE well. This is implemented as follows. As each hypershell is sampled, the minimum PE found within the hypershell is retained. As long as the minimum PE increases with subsequent hypershells,

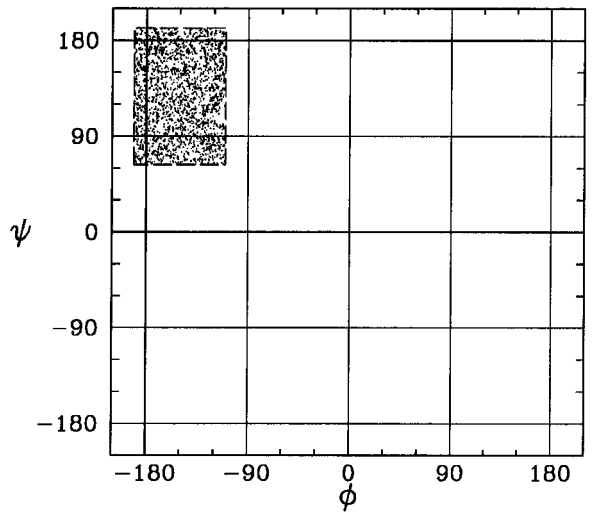

Figure 2. Monte Carlo integration of the first PE well. Dots mark the location of random conformations generated during MC integration of the PE well. For clarity, only 10% of the generated conformations are included in this figure.

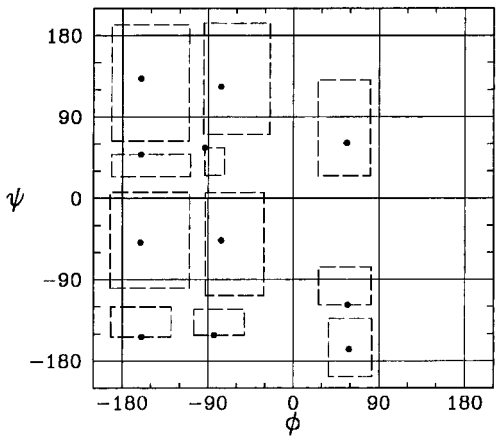

Figure 3. All PE wells found during mining minima calculations of alanine dipeptide. Dashed lines represent the extent of the 11 PE wells found for alanine dipeptide. The conformation of lowest energy within each well is identified by a filled circle. Strips between wells guard against double-counting any regions of phase space. Minimum energy structures that lie on the edge of dashed boxes represent "wells" which should more properly be considered "patches" on the sides of neighboring PE wells (see text).

the hypershells are considered to be contained within the current energy well. However, when the minimum PE of a hypershell is less than that of the previously sampled hypershell, that hypershell is considered to be associated with a different energy well and sampling within the current well therefore ceases.

The low-energy structures in the outermost hypershell define the extent of the PE well. The low-energy structures in successive hypershells around the global minimum of alanine dipeptide are shown in Figure 1. The rectangular extent of the associated PE well for this global minimum is represented by a dashed line.

Calculating the Free Energy of the PE Well. The free energy A_j of an individual PE well is computed by Monte Carlo integration, using eq 8. Random conformations are generated uniformly within the dihedral range specified by the extent of the PE well, as shown in Figure 2, and the unweighted average of the Boltzmann factor is computed for this region of phase space. The number of random conformations N_j is proportional to the volume of the well, with a minimum and maximum number of conformations specified by the user. The quality of convergence of the Monte Carlo integration within individual energy wells is examined in the Results and Discussion section.

Finding More Local Energy Minima. The entire procedure is iterated, with the restriction that trial conformations that fall within minima that have already been sampled are rejected. This prevents double-counting of energy minima and forces the algorithm to continue mining new energy wells. This method of excluding previously discovered minima can be viewed as a form of poling.[37]

The free energy is accumulated according to eq 7 as more minima are sampled. The process halts when the change of the cumulative free energy meets a user-specified convergence criterion. For the present illustration, 11 PE regions were sampled in order to converge the cumulative free energy of alanine dipeptide to within 1 ppm. The rectangular extents of these minima are shown as dashed lines in Figure 3. Because no attempts have been made to optimize this example calculation, not all of the PE regions represent unique minimum energy structures; some are "patches" on the side of a minimum PE well. This does not diminish the accuracy of the calculation, however, because the MC integration to compute A_j neither requires nor assumes harmonic energy wells. For ease of coding and to prevent double-counting of any regions of phase space, PE wells are separated by narrow gaps, as seen in Figure 3. The free energy contribution of these portions of phase space are accounted for by the $RT \ln(f_M)$ correction described below.

Computing the Fractional Occupancy. A Metropolis Monte Carlo simulation is performed, generating a Markov chain of accepted conformations. The step size is adjusted to yield an acceptance rate of approximately 50%. Each accepted conformation is checked to determine whether the conformation is in a region of conformational space corresponding to a minimum located by the mining-minima procedure just described. The fractional occupancy of these minima is computed and used to correct the predominant-states result according to eq 9.

Results and Discussion

Convergence and Timings for Oligopeptides and XK263. *Computational Details*. The methods detailed above have been applied to a series of alanine oligopeptides (**I**, $n = 1-5$, 7, 9), and to XK263 (**II**), an inhibitor of HIV-1 protease.[38,39] Free energies were computed both by MC integration over the full conformational phase space (eq 6) and by the mining-minima procedure.

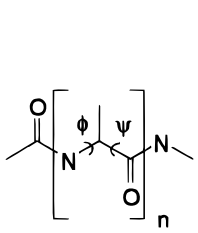

I

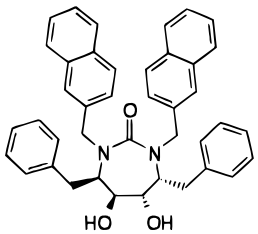

II

Initial coordinates for the alanine oligopeptides were generated by the program Quanta[40] in the all-*trans* conformation. For XK263, the coordinates of the protein-bound inhibitor were used directly.[38] All calculations used a locally modified version of UHBD[30] and the CHARMM 22 parameter set.[31] Oligopeptide structures were energy minimized briefly with nonbonded interactions turned off in order to establish a uniform set of bonds and angles. However, following this protocol for XK263 led to extreme steric overlap of ring substituents. Therefore,

TABLE 1: Calculated Free Energies for Alanine Oligopeptides and XK263[a]

		A_{MC} [kJ/mol]	A_{MM} [kJ/mol]	M	$RT\ln(f_M)$ [kJ/mol]	$A_{MM,corr}$ [kJ/mol]
Ala_2	$\epsilon = 1$	−188.51	−188.28	7	−0.20	−188.48
	$\epsilon = 25$	−10.85	−10.79	7	−0.28	−11.07
	ΔA	−177.66	−177.49			−177.41
Ala_3	$\epsilon = 1$	−310.52	−310.45	16	−0.24	−310.69
	$\epsilon = 25$	−22.01	−21.81	26	−0.46	−22.27
	ΔA	−288.51	−288.64			−288.42
Ala_4	$\epsilon = 1$	−433.85	−433.81	14	−0.22	−434.03
	$\epsilon = 25$	−34.06	−32.45	36	−1.79	−34.24
	ΔA	−399.79	−401.36			−399.79
Ala_5	$\epsilon = 1$	−555.07	−556.77	15	−0.90	−557.67
	$\epsilon = 25$	−46.73	−42.16	70	−5.11	−47.27
	ΔA	−508.34	−514.61			−510.40
Ala_6	$\epsilon = 1$	−669.73	−677.91	59	−2.56	−680.47
	$\epsilon = 25$	−58.83	−48.43	11	−12.72	−61.15
	ΔA	−610.90	−629.48			−619.32
Ala_8	$\epsilon = 1$	−912.64	−940.35	29	−1.59	−941.94
	$\epsilon = 25$	−83.01	−75.13	242	−13.56	−88.69
	ΔA	−829.63	−865.22			−853.25
Ala_{10}	$\epsilon = 1$		−1209.5	22	−9.8	−1219.3
	$\epsilon = 25$		−94.1	100	−22.7[b]	−116.8
	ΔA		−1115.4			−1102.5
XK263	$\epsilon = 1$	85.07	72.88	61	−0.37	72.51
	$\epsilon = 25$	209.52	201.83	35	−1.46	200.37
	ΔA	124.45	128.95			127.86

[a] A_{MC}, free energy computed by MC integration over complete conformational space; A_{MM}, free energy computed by the mining-minima procedure; M, number of minima sampled; $RT\ln(f_M)$, fractional occupancy correction to A_{MM}; $A_{MM,corr}$, $A_{MM} + RT\ln(f_M)$. [b] The calculation of $RT\ln(f_M)$ for alanine decapeptide has not converged; this value should therefore be regarded as unreliable.

the XK263 structure was minimized with electrostatic interactions turned off and van der Waals interactions turned on. MC integration and the mining-minima procedure were carried out for rotations of the ϕ and ψ backbone dihedral angles of the oligopeptides and for the 10 substituent dihedral angles of XK263. Oligopeptide methyl dihedrals and XK263 ring dihedrals were not sampled. A minimum of 2.5×10^3 and a maximum of 5.0×10^4 random conformations were generated during MC integration of individual minima located by the mining-minima procedure. Free energies for each molecule were computed with dielectric constants of 1 and 25.

MC Integration of Full Conformational Volume. Free energies computed by MC integration A_{MC} are listed in the first data column of Table 1. A number of general conclusions may be drawn from analysis of these calculations.

First, the calculations with a dielectric constant of 25 converge more quickly than the vacuum calculations. The left side of Figure 4 plots the computed free energy as a function of the number of MC samples for alanine dipeptide at $\epsilon = 25$ and $\epsilon = 1$. Note the difference in energy scales of the graphs. For alanine dipeptide, the $\epsilon = 25$ calculation yields good convergence with about half the number of MC samples required for the $\epsilon = 1$ calculation.

The chief reason the $\epsilon = 25$ calculations converge more quickly is illustrated in Figure 5. This figure presents two-dimensional projections of the potential energy landscape of alanine dipeptide, for $\epsilon = 25$ in the upper panels and for $\epsilon = 1$ in the lower panels. The points mark conformations located during the mining-minima calculations described below. The energy landscape shown for $\epsilon = 25$ varies relatively smoothly, and many conformations have similar energies. Thus, the MC calculation converges relatively easily. In fact, in the case of a perfectly flat landscape in which all conformations have the same energy, a single MC sample would suffice to compute the exact free energy.

In contrast, the $\epsilon = 1$ energy landscape is dominated by a single deep energy well, labeled A in Figure 5. Random conformations generated during MC integration must repeatedly sample this deep minimum in order for the computed free energy to converge. This difficulty is exacerbated as the system gets larger; the $\epsilon = 1$ energy landscape for larger oligopeptides is always dominated by a few deep minima that account for a very small portion of an ever-larger conformational phase space.

In addition, as might be expected, the free energy of small systems converges more rapidly than that of large systems. As shown in Figure 4, the free energy of alanine dipeptide appears well-converged after fewer than 2.0×10^6 steps of Monte Carlo integration. In contrast, even for the relatively smooth $\epsilon = 25$

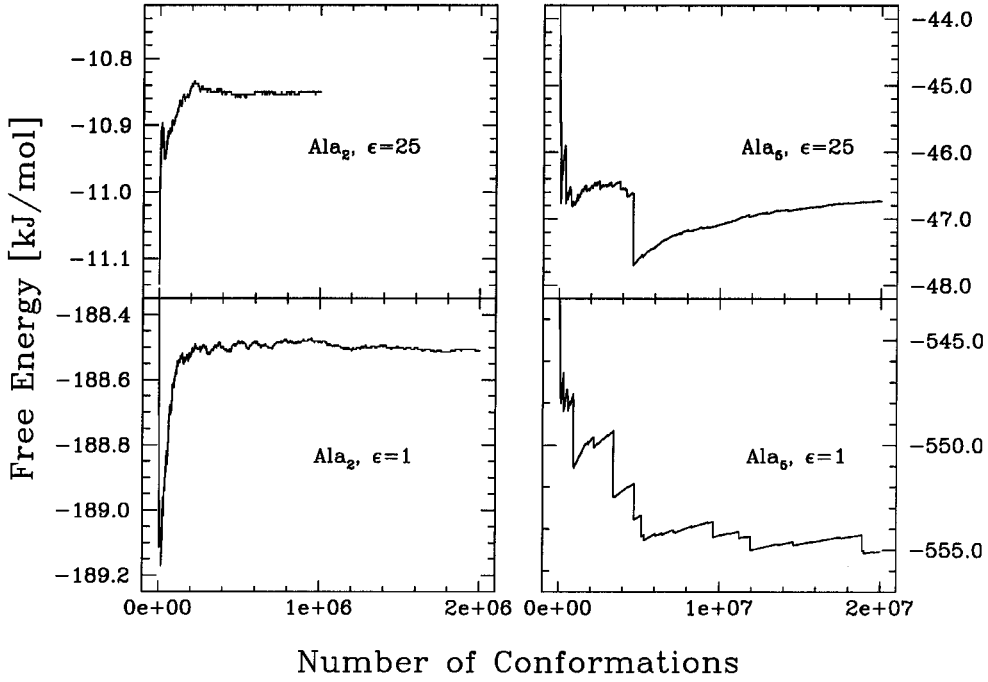

Figure 4. Convergence plots for Monte Carlo integration of alanine dipeptide and alanine pentapeptide at $\epsilon = 1$ and $\epsilon = 25$. Every ϕ and ψ dihedral angle was sampled in the range $[0, 2\pi]$.

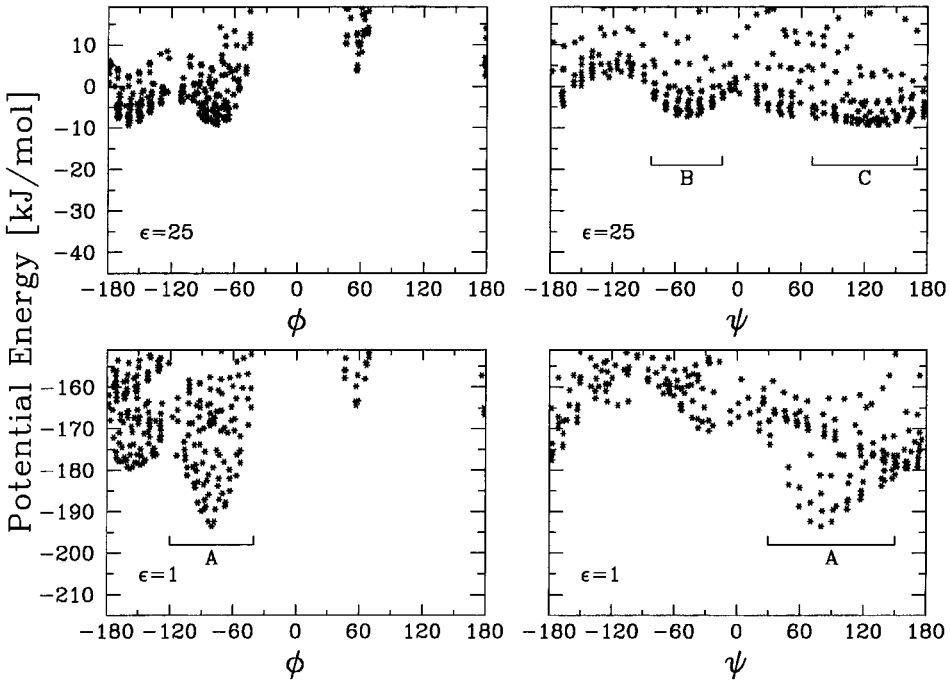

Figure 5. Potential energy surfaces of alanine dipeptide. Points mark structures located during mining-minima calculations at $\epsilon = 1$ and $\epsilon = 25$. The graphs on the left project all points onto the ϕ axis, and the graphs on the right project all points onto the ψ axis. See text for descriptions of labeled minima.

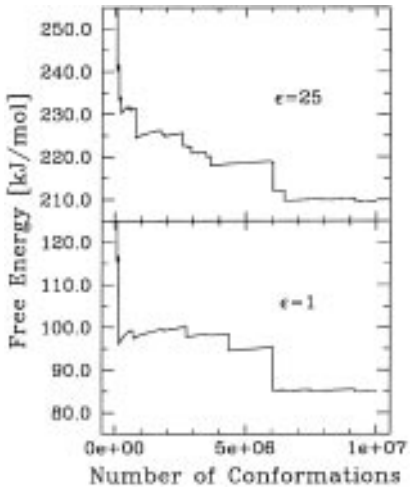

Figure 6. Convergence plots for Monte Carlo integration of XK263. Integrals range over $[0, \pi]$ for phenyl dihedrals and $[0, 2\pi]$ for all other substituent dihedral angles.

energy landscape, Monte Carlo integration of alanine pentapeptide has not converged in 2.0×10^7 steps. As the size of the system increases, this problem naturally becomes more severe. We therefore regard as unreliable the values of A_{MC} shown in Table 1 for peptides longer than Ala_4. As indicated by the gap in Table 1, we did not even attempt to compute A_{MC} for alanine decapeptide, with 18 dihedrals.

Finally, the MC integration method is very poorly suited for treating systems like XK263, in which large portions of conformational phase space have high energies due to van der Waals overlap between the large side chains. For this molecule, only a small portion of phase space makes a substantial contribution to the free energy, even when a high dielectric constant is used. This results in slow convergence of the MC integration, as illustrated in Figure 6.

"Mining-Minima" Results. The second and third columns of Table 1 list, respectively, the free energies computed by the mining-minima procedure, A_{MM}, and the number of minima sampled, M, for the oligopeptides and XK263. In all cases, minima were accumulated until the energies were converged to 1 ppm. An energy cutoff E_{cutoff} of 167 kJ/mol above the energy minimum $E_{min,j}$ was used for sampling hypershells in each PE well. Four conclusions may be drawn from analysis of these calculations.

First, in contrast to MC integration, the mining-minima method converges more quickly for the sharply peaked $\epsilon = 1$ potential energy surface than for the smooth $\epsilon = 25$ surface. In Figure 7, the cumulative free energy is plotted against the number of minima sampled. The free energy of alanine dipeptide is again shown on the left, with that of alanine pentapeptide on the right. The deep minimum labeled A in Figure 5 makes a dominant contribution to the free energy of alanine dipeptide. This energy minimum is located very early in the mining-minima process, and once it is sampled, additional minima make only small additional contributions to A_{MM}. On the other hand, for $\epsilon = 25$, the various minima are similar in energy, so a larger number must be sampled in order for convergence to be achieved. It is worth pointing out that the free energy yielded by the mining-minima method is an upper bound to the true result, barring numerical problems. As the MC integration within a single well progresses, the computed value of A_j can fluctuate. Convergence of the MC integration within individual wells is examined in more detail below. However, as the free energies of more minima are accumulated according to eq 7, the computed conformational free energy A_{MM} falls monotonically.

For small systems, free energies computed by the mining-minima method agree extremely well with free energies computed by MC integration, particularly for the sharply peaked $\epsilon = 1$ potential energy surface. For systems as large as alanine tetrapeptide—with six dihedral degrees of freedom—the value of $\Delta A \equiv A_{\epsilon=1} - A_{\epsilon=25}$ is essentially identical for both MC integration and the mining-minima calculation. The discrepancies found for larger molecules probably result from the poor convergence of the brute force MC calculations that yield A_{MC}.

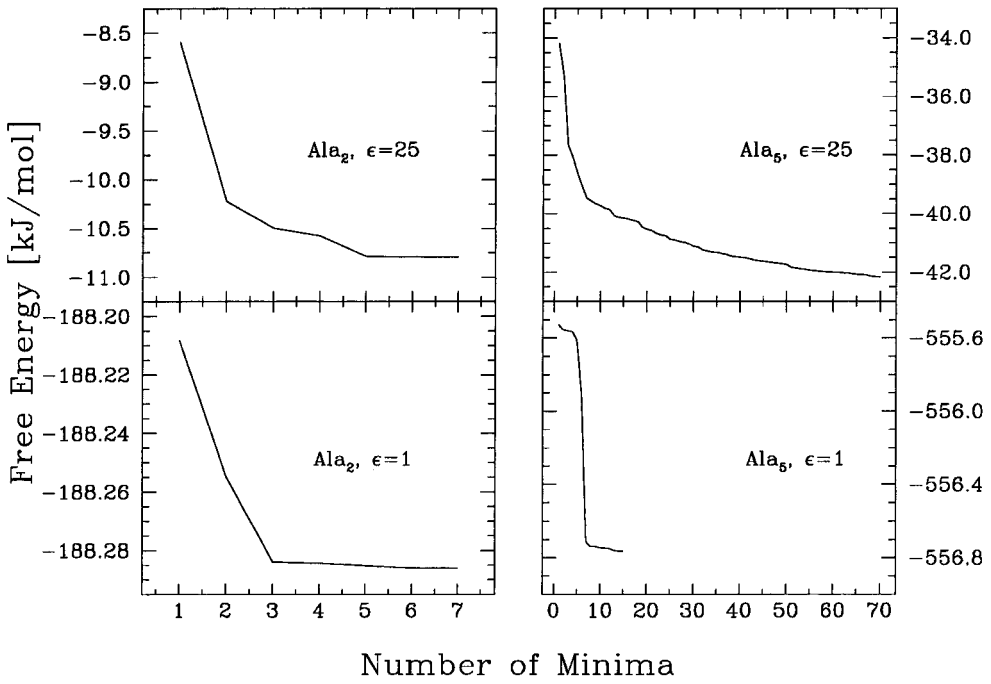

Figure 7. Convergence plots for mining-minima calculations of alanine dipeptide and alanine pentapeptide.

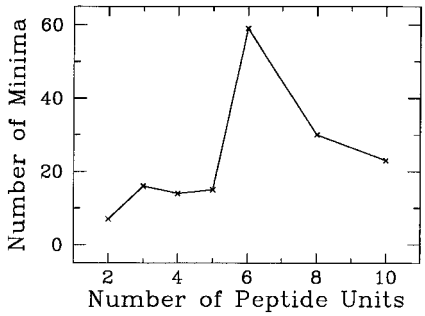

Figure 8. Number of minima required to converge A_{MM} of alanine oligopeptides to 1 ppm, with $\epsilon = 1$.

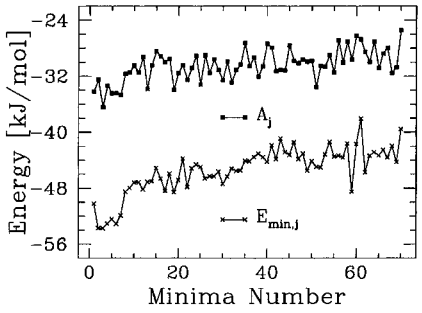

Figure 9. Sequence of energy wells of alanine pentapeptide found by the mining-minima method at $\epsilon = 25$. Crosses mark $E_{min,j}$ and filled squares mark A_j of each energy well.

Second, as was the case for MC integration, convergence is slower for larger systems. For example, obtaining converged results at $\epsilon = 25$ for alanine pentapeptide requires sampling 10 times as many minima as for alanine dipeptide (see Figure 7). In general, as the system size increases, more minima must be sampled in order to reach the same level of convergence.

However, an interesting exception to this general trend is illustrated in Figure 8. This figure plots the number of minima required to converge the $\epsilon = 1$ free energies to less than 1 ppm, as a function of the number of peptide units. Alanine hexapeptide requires roughly twice as many minima for convergence as predicted by interpolation between alanine pentapeptide and alanine octapeptide. The explanation is as follows. For these molecules at $\epsilon = 1$, the CHARMM potential energy surfaces of oligopeptides up to 5 units long are dominated by structures with repeating, ringlike $C7_{eq}$ units. For longer oligopeptides, α -helical structures predominate. The hexapeptide and, to a lesser extent, the octapeptide fall in the transition between these two regimes. As a consequence, many largely α -helical conformations are similar in energy to conformations with repeating $C7_{eq}$ units. Therefore, all these minima must be sampled to achieve convergence. Remarkably, this change in preferred conformation is consistent with results of more elaborate FEP calculations using explicit solvent molecules.[41]

Third, the mining-minima procedure tends to sample minima in order of increasing potential energy. This reflects the success of the technique used for finding energy minima and the fact that each minimum can be sampled only once. This result is illustrated for alanine pentapeptide at $\epsilon = 25$ in the lower portion of Figure 9.

TABLE 2: Comparison of Second and Third Minima Found for Alanine Pentapeptide at $\epsilon = 25$[a]

	minimum 2	minimum 3
$E_{min,j}$ [kJ/mol]	−53.71	−53.72
A_j [kJ/mol]	−32.49	−36.46
ϕ_1	−76°	−77°
ψ_1	−42°	−33°
ϕ_2	−76°	−74°
ψ_2	−21°	−34°
ϕ_3	−72°	−70°
ψ_3	−34°	−35°
ϕ_4	−163°	−165°
ψ_4	−59°	−110°

[a] $E_{min,j}$, minimum potential energy within well; A_j, free energy of well.

However, increasing potential energy does not necessarily imply increasing *free* energy, as illustrated by comparison with the upper portion of Figure 9. For example, the second and third minima found for alanine pentapeptide have virtually identical potential energies $E_{min,j}$, but their free energies A_j differ by about 4 kJ/mol, as shown in Table 2. In addition, the conformations at the two energy minima are quite similar. The chief conformational difference is that ψ_4 changes from −60° to 110°. The difference in free energies can be rationalized by

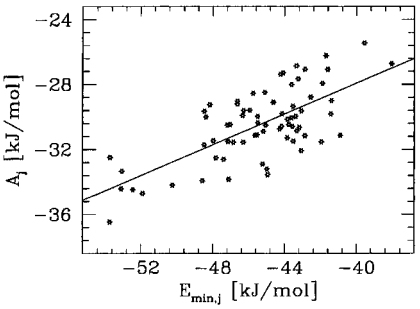

Figure 10. Free energy A_j versus potential energy $E_{\min,j}$ for energy wells of alanine pentapeptide at $\epsilon = 25$. This scatter plot graphs the energies shown in Figure 9. The straight line is a least squares fit to the data, with a correlation coefficient of 0.70.

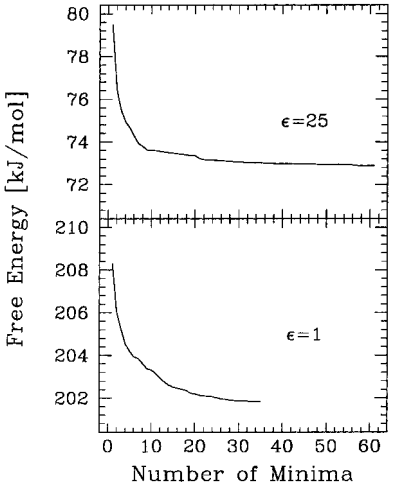

Figure 11. Convergence plots for mining-minima calculations of XK263 at $\epsilon = 1$ and $\epsilon = 25$.

reference to the potential energy surfaces of alanine dipeptide (Figure 5). Energy minimum 3 of the pentapeptide has $\psi_4 \approx 110$, corresponding to the broad minimum labeled C, and therefore has a relatively low free energy. In contrast, energy minimum 2 corresponds to the narrower well with $\psi \approx -60$, labeled B.

It is of interest to examine the correlation between potential energy and free energy. As shown in Figure 10, there is a significant correlation between $E_{\min,j}$ and A_j for the energy wells at $\epsilon = 25$ for alanine pentapeptide. The slope of the least squares fit is 0.47, implying that as $E_{\min,j}$ rises, the width of the energy well increases. However, the correlation between $E_{\min,j}$ and A_j is far from perfect. Similar correlations are seen for all of the systems studied here (data not shown). This result highlights the importance of examining not only the depth of each PE well but also its shape and breadth.

Fourth, the mining-minima procedure is ideally suited to systems like XK263. Precisely the same features that make this system a challenge for the simple MC integration method make it appropriate for the mining-minima procedure. The procedure quickly locates and samples the narrow energy wells, yielding excellent convergence, as seen in Figure 11.

MC Integration of Individual Minima. Convergence plots are shown in Figure 12 for MC integrals within the 15 energy wells located for alanine pentapeptide at $\epsilon = 1$ (see previous subsection). Within each well, 5×10^4 random conformations were generated. The convergence is excellent for most of the wells. It is clear that restricting the limits of integration to areas of low energy drastically improves convergence of the calculation, compared with the MC integrals in the entire conformational space (see Figure 4).

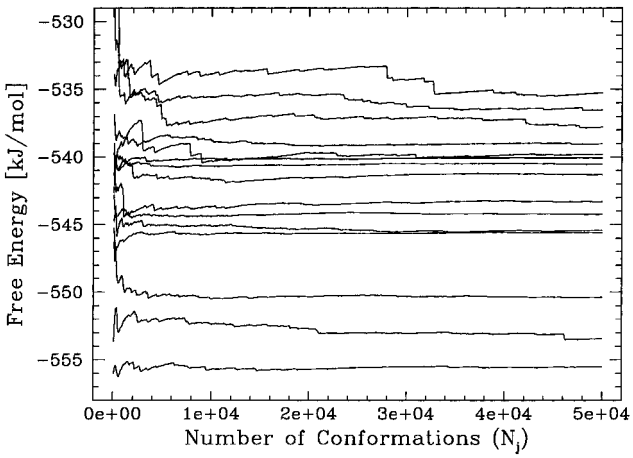

Figure 12. Convergence plots for Monte Carlo integration within individual PE wells of alanine pentapeptide at $\epsilon = 25$.

TABLE 3: Approximate CPU Times for Free Energy Calculations of Alanine Oligopeptides and XK263[a]

		A_{MC}		A_{MM}		$RT \ln(f)$
		N	CPU [min]	M	CPU [min]	CPU [min]
Ala_2	$\epsilon = 1$	2.0×10^6	55	7	2.0	1.5
	$\epsilon = 25$	1.0×10^6	27	7	2.6	1.5
Ala_3	$\epsilon = 1$	1.0×10^7	480	16	110	5.6
	$\epsilon = 25$	1.0×10^7	540	26	190	11
Ala_4	$\epsilon = 1$	3.5×10^7	2700	14	150	27
	$\epsilon = 25$	2.0×10^7	1700	36	470	35
Ala_5	$\epsilon = 1$	2.0×10^7	2200	15	370	170
	$\epsilon = 25$	2.0×10^7	2300	70	1100	100
Ala_6	$\epsilon = 1$	1.0×10^7	2400	59	1200	270
	$\epsilon = 25$	1.0×10^7	1700	11	240	190
XK263	$\epsilon = 1$	1.0×10^7	3000	61	1300	240
	$\epsilon = 25$	1.0×10^7	3000	35	1700	700

[a] *N*, number of randomly sampled conformations; CPU times measured on an SGI R4400 Indigo^2 workstation. See Table 1 for other symbols.

On the other hand, not all of the free energies are perfectly converged; see especially the top plot of Figure 12. In the present case, this lack of convergence has little effect upon the final results, because it occurs in a high-energy well that contributes little to the configuration integral. It should be possible to minimize such convergence problems by applying an appropriate convergence criterion. Although this would require additional computer time for some energy wells, it should speed the calculations for the more common case in which the integral converges rapidly (see Figure 12).

Correction for Other Conformations by Fractional Occupancy. A weakness of the mining-minima procedure is that, by itself, it neglects free energy contributions from conformations that do not lie in the deepest energy minima. In a system with many degrees of freedom, these other conformations can contribute significantly. Their contribution is assessed here through the use of eq 9, and the results are listed in Table 1.

As shown, even systems as small as alanine dipeptide have a noticeable contribution from $RT \ln(f_M)$. As one would expect, in general the correction is larger for $\epsilon = 25$, resulting from smoother pseudosolvent landscapes with many roughly equivalent minima. As system size becomes large, it again becomes difficult to converge the Metropolis Monte Carlo calculations of f_M (results not shown). It is likely that a more efficient MC algorithm, such as a configuration-biased method,[42−46] will yield improved convergence.

CPU Timings. Approximate CPU timings, in minutes, are listed in Table 3. The CPU times for the MC integration method

are significantly longer than those for the mining-minima procedure, even though the results of the MC integration method are not reliably converged. Moreover, the mining-minima method has not yet been optimized for speed.

Conformational Preferences of Substituted Cyclic Ureas. The cyclic urea inhibitors of HIV-1 protease possess four different stable ring conformations. The mining-minima method is used here to assess the relative stability of these conformations for three cyclic ureas with different substituents.

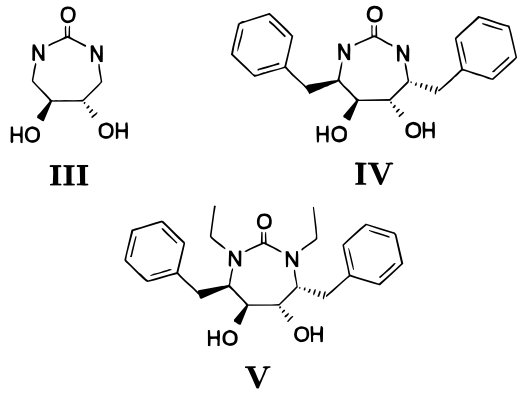

III IV

V

Computational Details. Four stable ring structures of 5,6-dihydroxy cyclic urea were identified by high-temperature molecular dynamics followed by energy minimization. The ring may adopt either pseudoboat or pseudochair conformations. In either case, the two hydroxy substituents on the ring may be either axial or equatorial to the ring. There are thus four distinct ring conformations. These will be referred to according to ring conformation and hydroxyl orientation, *e.g.*, the boat-axial structure.

Benzyl and ethyl substituents were built onto each of the four stable cyclic urea structures using Quanta.[40] The 12 resulting structures were minimized briefly to relieve bad steric contacts and to optimize bonds and angles. The mining-minima procedure was used to sample over the dihedral angles of the substituents of the ring and thus to compute the conformational free energy of each stable ring structure. Methyl dihedrals were sampled over the range $[0, 2\pi/3]$; phenyl dihedrals were sampled over the range $[0, \pi]$, and all other substituent dihedrals were sampled over the range $[-\pi, \pi]$. Cumulative free energies for each molecule were converged to 0.1 ppm. All calculations used the CHARMM 22 parameter set[31] and a distance-dependent dielectric, $\epsilon = 4r$.

The results of these calculations are listed in Table 4. The reported free energy values include $RT \ln(f_M)$ corrections. However, these corrections were small: less than 0.4 kJ/mol for the dihydroxy and dibenzyl, dihydroxy substituted ureas and less than 2.4 kJ/mol for the dibenzyl, diethyl, dihydroxy substituted urea.

5,6-Dihydroxy Cyclic Urea. The most stable conformation of the cyclic urea core is predicted to be the pseudoboat ring conformation in which the dihydroxy substituents are in an axial orientation. Ten energy wells sufficed to converge the free energy to within 0.1 ppm.

4,7-Dibenzyl-5,6-dihydroxy Cyclic Urea. Dibenzyl substitution at the 4,7 positions favors the chair-axial conformation of the ring. This conformation positions the dibenzyl substituents away from the cyclic urea core. Part of the reason this conformation is stable is that its minimum PE is lower than those of the other three ring conformations. In addition, the chair-axial conformation has a large number of PE wells of similar free energy: 65 minima were required to converge the free energy of this conformation, while fewer than 30 minima were required to converge the free energies of the less stable ring conformations.

4,7-Dibenzyl-1,3-diethyl-5,6-dihydroxy Cyclic Urea. Addition of diethyl substituents on the cyclic urea nitrogens favors the chair-equatorial conformation. Sixty-five minima were required to converge the cumulative free energy to 0.1 ppm. In contrast to 4,7-dibenzyl substitution, the most stable ring conformation in this case has fewer PE wells of similar free energy than do the less stable ring conformations. Favorable van der Waals interactions between benzyl and ethyl substituents may help to stabilize the chair-equatorial ring conformation.

Implications. The conformational preferences presented here are consistent with experimental analyses of these and related molecules by X-ray crystallography and NMR spectroscopy.[47,48] This could be coincidental, given that the present calculations treat environmental effects crudely. Nonetheless, the results are encouraging.

This problem would be challenging for perturbative methods of computing free energies, because it would be necessary to force the ring in steps from one stable conformation to another, equilibrating the system at each step. This could be difficult, due to the high-energy barriers between stable conformations of the ring. With the present method, it is necessary only to compute the free energies of the four stable conformations.

Conclusions

The mining-minima procedure described here allows direct computation of conformational free energy for systems with modest numbers of torsional degrees of freedom. No assumptions are made concerning the number or nature of low-energy states. In particular, it is not necessary to assume that the energy

TABLE 4: Calculated Free Energies for Substituted Cyclic Ureas[a]

	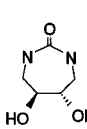		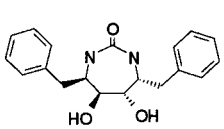		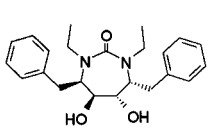	
	$A_{MM,corr}$ $[kJ/mol]$	M	$A_{MM,corr}$ $[kJ/mol]$	M	$A_{MM,corr}$ $[kJ/mol]$	M
boat-axial	54.49	10	88.64	22	123.7	87
boat-equitorial	60.78	9	98.23	29	123.3	74
chair-axial	60.92	10	76.06	65	121.3	96
chair-equitorial	74.02	10	102.54	26	105.2	65

[a] See Table 1 for symbols.

wells are harmonic or that they all have the same shape. The new method is particularly useful for systems whose configuration integrals are dominated by a few low-energy conformations. However, the method may still be used for systems that do not meet this criterion because an additional Monte Carlo calculation can be used to correct for conformations not included in the sum over energy minima.

The method yields excellent convergence and good agreement with experiment when applied to a series of druglike, synthetic ligands of HIV-1 protease. It is anticipated that this procedure will also be useful in computing the free energy of binding of small molecules with synthetic hosts and perhaps with protein receptors. This application will require sampling over the external position and orientation of a molecule in addition to its internal degrees of freedom. The procedure is currently being adapted for this purpose.

The free energy calculations presented here utilize the CHARMM parameter set and a simple treatment of solvent effects. However, the method can be used with any fast energy and solvation model. Moreover, the basic steps of the algorithm—finding and integrating over new minima and computing the fractional occupancy of the minima that have been sampled—could be implemented with a variety of other algorithms. For example, distance-geometry methods could be used to rapidly locate conformations that might be in or near important energy minima. Also, as noted above, the Metropolis Monte Carlo method probably is not optimal for computing f_M. Finally, an alternative formulation of the mining-minima approach, not presented here, is readily parallelizable. This should permit even faster free energy calculations on parallel supercomputers.

Acknowledgment. This project is supported by the National Institutes of Health (GM54053), the National Institute of Standards and Technology, and the Center for Advanced Research in Biotechnology. M.S.H. is a National Research Council Research Associate. We thank Dr. Hillary S. R. Gilson of the Center for Advanced Research in Biotechnology for helpful conversations and Dr. C. Nicholas Hodge of the DuPont Merck Pharmaceutical Company for helpful conversations and for providing unpublished experimental data. No approval or endorsement of any commercial product by the National Institute of Standards and Technology is intended or implied.

References and Notes

(1) Wong, C. F.; McCammon, J. A. *J. Am. Chem. Soc.* **1986**, *108*, 3830−3832.
(2) Bash, P.; Singh, U. C.; Langridge, R.; Kollman, P. A. *Science* **1987**, *236*, 564−568.
(3) Beveridge, D. L.; DiCapua, F. M. *Annu. Rev. Biophys. Biophys. Chem.* **1989**, *18*, 431−492.
(4) Lybrand, T. P. In *Reviews in Computational Chemistry*; Lipkowitz, K. B., Boyd, D. B., Eds.; VCH: New York, 1990; Vol. 1, pp 295−320.
(5) Straatsma, T. P.; McCammon, J. A. *Annu. Rev. Phys. Chem.* **1992**, *43*, 407−435.
(6) Warshel, A.; Tao, H.; Fothergill, M.; Chu, Z.-T. *Isr. J. Chem.* **1994**, *34*, 253−256.
(7) Gilson, M. K.; Honig, B. *Proteins: Struct., Funct., Genet.* **1988**, *4*, 7−18.
(8) Kang, Y. K.; Gibson, K. D.; Némethy; Scheraga, H. A. *J. Phys. Chem.* **1988**, *92*, 4739−4742.
(9) Wesson, L.; Eisenberg, D. *Protein Sci.* **1992**, *1*, 227−235.
(10) Honig, B.; Sharp, K.; Yang, A.-S. *J. Phys. Chem.* **1993**, *97*, 1101−1109.
(11) Stouten, P. F. W.; Frömmel, C.; Nakamura, H.; Sander, C. *Mol. Simul.* **1993**, *10*, 97−120.
(12) Cramer, C. J.; Truhlar, D. G. In *Reviews in Computational Chemistry*; Lipkowitz, K. B., Boyd, D. B., Eds.; VCH: New York, 1995; Vol. 6, pp 1−72.
(13) June, R. L.; Bell, A. T.; Theodorou, D. N. *J. Phys. Chem.* **1990**, *94*, 1508−1516.
(14) Maginn, E. J.; Bell, A. T.; Theodorou, D. N. *J. Phys. Chem.* **1995**, *99*, 2057−2079.
(15) Lipkowitz, K. B.; Demeter, D. A.; Zegarra, R.; Larter, R.; Darden, T. *J. Am. Chem. Soc.* **1988**, *110*, 3446−3452.
(16) Lipkowitz, K. B.; Zegarra, R. *J. Comput. Chem.* **1989**, *10*, 595−602.
(17) Wang, J.; Szewczuk, Z.; Yue, S.-Y.; Tsuda, Y.; Konishi, Y.; Purisima, E. O. *J. Mol. Biol.* **1995**, *253*, 473−492.
(18) Wang, J.; Purisima, E. O. *J. Amer. Chem. Soc.* **1996**, *118*, 995−1001.
(19) Phillips, A. T.; Rosen, J. B.; Walke, V. H. *Dimacs Series in Discrete Mathematics and Theoretical Computer Science*; American Mathematical Society: Providence, RI, 1995, Vol. 23, pp 181−198.
(20) Gilson, M. K. *Proteins: Struct., Funct., Genet.* **1993**, *15*, 266−282.
(21) Vieth, M.; Kolinski, A.; Skolnick, J. *J. Chem. Phys.* **1995**, *102*, 6189−6193.
(22) Vieth, M.; Kolinski, A.; Brooks, C. L., III; Skolnick, J. *J. Mol. Biol.* **1995**, *251*, 448−467.
(23) Hill, T. L. *Cooperativity Theory in Biochemistry*, 1st ed.; Springer Series in Molecular Biology; Springer-Verlag: New York, 1985.
(24) Gilson, M. K.; Given, J. A.; Bush, B. L.; McCammon, J. A. *Biophys. J.*, in press.
(25) Pitzer, K. S. *J. Chem. Phys.* **1946**, *14*, 239−243.
(26) Chandler, D.; Pratt, L. R. *J. Chem. Phys.* **1976**, *65*, 2925−2940.
(27) Mayer, J. E.; Brunauer, S.; Mayer, M. G. *J. Am. Chem. Soc.* **1933**, *55*, 37−53.
(28) Press, W. H.; Flannery, B. P.; Teukolsky, S. A.; Vetterling, W. T. *Numerical Recipes: The Art of Scientific Computing;* Cambridge University Press: London, 1986.
(29) Metropolis, N.; Rosenbluth, A. W.; Rosenbluth, M. N.; Teller, A. H.; Teller, E. *J. Chem. Phys.* **1953**, *21*, 1087−1091.
(30) Davis, M. E.; Madura, J. D.; Luty, B. A.; McCammon, J. A. *Comput. Phys. Commun.* **1991**, *62*, 187−197.
(31) Brooks, B. R.; Bruccoleri, R.; Olafson, B. D.; States, D. J.; Swaminathan, S.; Karplus, M. *J. Comput. Chem.* **1983**, *4* (2), 187−217.
(32) Davis, L. *Handbook of Genetic Algorithms;* Van Nostrand Reinhold: New York, 1991.
(33) Lucasius, C. B.; Kateman, G. *Chemom. Intell. Lab. Syst.* **1993**, *19*, 1−33.
(34) Judson, R. S.; Jaeger, E. P.; Treasurywala, A. M. *J. Mol. Struct. (THEOCHEM)* **1994**, *308*, 191−206.
(35) Judson, R. S.; Jaeger, E. P.; Treasurywala, A. M.; Peterson, M. L. *J. Comput. Chem.* **1993**, *14*, 1407−1414.
(36) Herrmann, F.; Suhai, S. *J. Comput. Chem.* **1995**, *16*, 1434−1444.
(37) Smellie, A.; Teig, S. L.; Towbin, P. *J. Comput. Chem.* **1995**, *16*, 171−187.
(38) Lam, P. Y. S.; Jadhav, P. K.; Eyermann, C. J.; Hodge, C. N.; Ru, Y.; Bacheler, L. T.; Meek, J. L.; Otto, M. J.; Rayner, M. M.; Wong, Y. N.; Chang, C.-H.; Weber, P. C.; Jackson, D. A.; Sharoe, T. R.; Erickson-Vitanen, S. *Science* **1994**, *263*, 380−384.
(39) Hodge, C. N.; Aldrich, P. E.; Bacheler, L. T.; Chang, C.-H.; Eyermann, C. J.; Garber, S.; Grubb, M.; Jackson, D. A.; Jadhav, P. K.; Korant, B.; Lam, P. Y. S.; Maurin, M. B.; Meek, J. L.; Otto, M. J.; Rayner, M. M.; Reid, C.; Sharpe, T. R.; Shum, L.; Winslow, D. L.; Erickson-Vitanen, S. *Chem. Biol.* **1996**, *3*, 301−314.
(40) Molecular Simulations Inc., Waltham, MA.
(41) Wang, L.; O'Connell, T.; Tropsha, A.; Hermans, J. *Proc. Natl. Acad. Sci. U.S.A.* **1995**, *92*, 10924−10928.
(42) Rosenbluth, M. N.; Rosenbluth, A. W. *J. Phys. Chem.* **1955**, *23*, 356−359.
(43) Frenkel, D.; Mooij, G. C. A. M.; Smit, B. *J. Phys. Condens. Matter* **1991**, *4*, 3053−3076.
(44) Guarnieri, F.; Still, W. C. *J. Comput. Chem.* **1994**, *15*, 1302−1310.
(45) Senderowitz, H.; Guarnieri, F.; Still, W. C. *J. Am. Chem. Soc.* **1995**, *117*, 8211−8219.
(46) Deem, M. W.; Bader, J. S. *Mol. Phys.* **1996**, *87*, 1245−1260.
(47) Lam, P. Y. S.; et al. *J. Med. Chem.* **1996**, *39*, 3514−3525.
(48) Hodge, C. N. Personal communication. Dr. Hodge and co-workers have a detailed conformational and SAR analysis in press.